

*Received October 11, 2015; reviewed; accepted July 27, 2016*

## INFLUENCE OF DRY GRINDING ON PHYSICOCHEMICAL AND SURFACE PROPERTIES OF TALC

Zeyni ARSOY\*, Bahri ERSOY\*, Atilla EVCIN\*\*, Mehmet G. ICDUYGU\*\*\*

\* Afyon Kocatepe University, Department of Mining Engineering, 03200 Afyonkarahisar, Turkey  
bersoy@aku.edu.tr & bahriersoy@yahoo.com

\*\* Afyon Kocatepe University, Department of Materials Science & Engineering, 03200 Afyonkarahisar, Turkey

\*\*\* Giresun University, School of Civil Aviation, 28200 Giresun, Turkey

**Abstract:** In this study the effect of dry grinding on hydrophobicity, surface free energy (*SFE*), particle size distribution, surface area, porosity, oil absorption, and whiteness of talc was investigated. The dry grinding was performed in a vibrating ball mill at various grinding times (5-150 min) by keeping the grinding parameters constant such as the number of ball, ball size, the amount of talc, vibration frequency and amplitude. Then, the contact angle measurements were performed on disc-shaped samples produced under a hydraulic press by using a sessile drop method with different liquids (water, formamide, diiodomethane, and ethylene glycol), and surface free energies ( $\text{mJ}/\text{m}^2$ ) were calculated according to OCG-AB (van Oss-Chaudhury-Good Acid-Base) method by using the obtained contact angle values. In addition, the physicochemical analyses given above were carried out for each ground sample. According to the obtained results, the water contact angle and *SFE* of the original sample were  $63.80^\circ$  and  $48.70 \text{ mJ}/\text{m}^2$ , respectively. The lowest and highest contact angle values for the samples were obtained as  $59.30^\circ$  and  $70.77^\circ$  at grinding times for 5 and 15 min, respectively. It was also determined that the grinding time over 30 min showed no significant effect on the contact angle and *SFE* values of the samples. Similarly, the grinding time vs. *SFE*, and the grinding time vs. contact angle curves showed a similar trend. Parallel to the increase in the surface area upon the grinding, a small increase in the oil absorption and whiteness of talc was also determined.

**Keywords:** talc, grinding, contact angle, surface free energy, oil absorption, whiteness

### Introduction

Talc is a hydrated magnesium silicate with a theoretical formula of  $\text{Mg}_3(\text{Si}_2\text{O}_5)_2(\text{OH})_2$ . Ideally, it contains 31.70% MgO, 63.50%  $\text{SiO}_2$ , and 4.80% water (Grim, 1968). Primary properties of talc can be summarized as follows: natural hydrophobicity, organophilicity, lamellar structure with a high aspect ratio (the length of basal surface

of layer/thickness of edge surface of layer), softness, low electrical conductivity, thermal resistance, and oil/surfactant/polymer adsorption ability (Grim, 1968; Van Olphen, 1977; Sanchez-Soto et al., 1997; Tomaino, 2000; Lopez-Galindo et al., 2004; Yekeler et al., 2004; Perez – Rodriguez and Sanchez – Soto, 1991; Cawood et al., 2005; Liu et al., 2006; Wang and Somasundaran, 2005; Nkoumbou, 2008; Wallqvist, 2009). Because of these properties, talc is used in many different industries such as ceramic, paint, cosmetic, paper, food, plastic, textile (Tomaino, 2000; Lopez-Galindo et al., 2004; Bizi et al., 2003; Martin et al., 2004; Goren et al., 2006; Neto and Moreno, 2007; Terada and Yonemochi, 2004).

In order to use talc in the mentioned industries, it is necessary to convert talc into powder by grinding. The previous studies showed that mechanical effects (impact, shear, and compression) and heat treatment during the grinding process deforms crystal structure of minerals, and minerals can even lose their crystallinity (Perez–Rondriquez and Sanchez–Soto, 1991; Tarada and Yonemochi, 2004; Lio and Senna, 1992; Filio et al., 1993; Aglietti, 1994; Kano and Saito, 1998; Temujin et al., 2003; Yang et al., 2006; Balek et al., 2007; Dellisanti et al., 2009). Serious changes have been detected in physical (grain shape, aspect ratio, roughness, specific surface area, particle size distribution, color, and cation exchange capacity) (Sanchez-Soto et al., 1997; Yekeler et al., 2004; Dellisanti et al., 2009; Zbik et al., 2005; Ulusoy, 2008), and surface properties (surface energy, hydrophobicity, and wettability) after the grinding process (Wu et al., 1996; Liao and Senna, 1992; Yekeler et al., 2004).

Hydrophobicity and surface free energy (*SFE*) concepts are encountered in many industries such as mining, oil, paper, pharmaceutical, paint, environment, textile, food, agriculture, and metal (Leja, 1982; Good and Van Oss 1992; Fowkes, 1964; Fowkes, 1972; Yoon and Yordan 1991; Gonul, 2000; Kolluri, 1994). There are a few studies investigating the changes in surface energy and hydrophobicity of talc after the grinding process in the literature. In a PhD study carried out by Yildirim (2001), contact angle of talc samples, which belong to different regions of the USA was determined by using the thin layer wicking (TLW) method, and surface free energies of those samples were measured by heat of wetting method using a micro-calorimeter. It was observed that the *SFE* of talc samples changed between 21.60 mJ/m<sup>2</sup> and 48 mJ/m<sup>2</sup>, and decreased with the decreasing particle size while there was an increase in the hydrophobicity with the decreasing particle size. Yildirim (2001) explained this change by fracture of talc along layer planes, and increase with the ratio of basal surface area to total surface area. However, in a different study by Terada and Yonemochi (2004), it was indicated that SFE of talc samples ground for different periods (3, 10, and 40 min) in a vibrating ball mill increased with the increasing grinding time, and it started to decrease after 10 min. Yekeler et al. (2004) investigated the effect of different grinding methods (ball, rod, and autogenous) on surface properties (grain shape, surface roughness, wettability, and surface energy) of talc. It was observed that talc ground by rod mill showed smoother surface, lower surface

energy, and higher water contact angle compared to talc ground by other grinding methods.

Fillers used in industries such as paint, paper, and plastic must satisfy certain requirements. In practice, raw materials used in plastic industry should have high hydrophobic property while a good dispersion of raw materials in water is desired in paint and paper industries. However, there is no study in the literature dealing with the hydrophobicity of talc used as a filler, especially in paint and paper industries. In a study conducted by Lefebvre et al. (2011), wettability and dispersion of talc in aqueous systems were investigated by coating talc surface with hydrophobic silica (Aerosil R972®). Their results showed that the coating process increased the hydrophobicity, and thus decreased wettability and dispersability of talc. However, the authors indicated that dispersion problem in aqueous environments created by high hydrophobicity could be overcome by using high speed mixing procedure (1500 rpm or higher).

In this study, the effect of grinding time on surface and various physical properties of talc sample, which was ground by a vibrating mill used in industry for ultrafine grinding processes was investigated in detail. The aim of this work was to prepare ground talc with desired particle size (around 5-20  $\mu\text{m}$ ) and maximum basal surface area. In other words, it was intended to obtain talc samples with maximum aspect ratio values (thus maximum hydrophobicity) in order to improve opacity of end-product (talc) used in industries such as paint, paper, etc.

## Experimental

### Material

A talc sample used in the experiments was obtained from the talc deposit which belongs to Ulusoy Mining Co. located 53 km from Sivas in Turkey. First, the size reduction procedures were applied to get appropriate size ( $-1\text{ mm}$ ) for the grinding processes. This talc sample was assigned as an original sample with T0 code for the rest of the grinding processes. The mineralogical analysis of the sample was performed by using a Shimadzu XRD-6000 instrument with  $\text{CuK}\alpha$  radiation and X-ray spectrum of the sample, and the results are seen in Fig. 1. As can be seen from the spectrum in Fig. 1., all peaks belong to talc mineral, and the sample showed high purity. The chemical analysis of the sample was carried out in a XRF (Bruker S8 Tiger) instrument, and the results are presented in Table 1. The specific density of original sample was recorded in a helium pycnometer (Quantachrome Ultrapycnometer 1000e) as  $2.80\text{ g/cm}^3$ , and the moisture content of the sample was determined as 1.08% (Denver IR-30). The liquids used for the contact angle measurements were of Merck Quality, and their specifications are presented in Table 2.

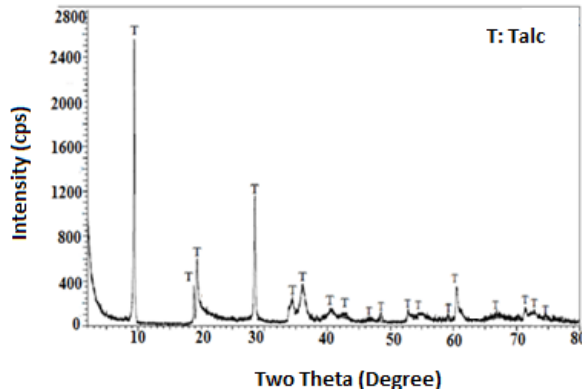
Fig. 1. Mineralogical (XRD) analysis of talc sample ( $Mg_3Si_4O_{10}(OH)_2$ )

Table 1. Chemical analysis of talc sample

Composition	SiO <sub>2</sub>	MgO	Fe <sub>2</sub> O <sub>3</sub>	Al <sub>2</sub> O <sub>3</sub>	CaO	NiO	CuO	LOI
Amount (%)	59.31	33.15	0.43	0.05	0.05	0.04	0.03	6.92

Table 2. Properties of polar and apolar liquids used for *SFE* calculations

Liquid	Chemical structure	Purity (%)	Molecular weight (g/mol)	Surface tension/energy components		
				$\gamma$	$\gamma^{LW}$	$\gamma^{AB}$
Water	H <sub>2</sub> O	Ultra pure	18.015	72.80	21.80	51.00
Diiodomethane	CH <sub>2</sub> I <sub>2</sub>	>99%	267.84	50.80	50.80	0.00
Formamide	CH <sub>3</sub> NO	>98%	45.04	58.00	39.00	19.00
Ethylene Glycol	HOCH <sub>2</sub> CH <sub>2</sub> OH	>99%	62.07	48.00	29.00	19.00

$\gamma$  = Total surface tension (or energy) (mJ/m<sup>2</sup>);

$\gamma^{LW}$  = Lifshitz-Van der Walls (LW) component;

$\gamma^{AB}$  = Lewis Acid-Base component

## Methods

Original talc sample with -1 mm particle size was ground in a vibrating ball mill (Siebtechnik GSM 06) at various grinding times (5, 10, 15, 30, 60, 90, 120, and 150 min) by using parameters given in Table 3. In the grinding processes conducted with the vibrating mills, the impact, shear, and compression forces can be affective, depending on the grinding medium. Meanwhile, the ceramic balls were used to eliminate metal contamination during the grinding process. After each grinding time, the particle size distribution (Malvern Mastersizer 2000), specific surface area (Quantachrome Nova 2200), pore volume (Quantachrome Nova 2200), and color (Datacolor Elrepho 3000) analyses were performed for the ground samples.

Table 3. Equipment and grinding medium properties of vibrating ball mill and grinding parameters for talc

Properties	Values
Chamber volume (cm <sup>3</sup> )	500
Vibration amplitude (mm)	0-6
Vibration intensity (rpm)	1500
Grinding period (min)	5-150
Ball diameter (mm)	13-14
Ball density (g/cm <sup>3</sup> )	2.47
Ball charge (%)	80
Density (g/cm <sup>3</sup> )	2.8
Bulk density (g/cm <sup>3</sup> )	0.76
Charge load (%)	20
Charge load (g)	152.16
$d_{10}$ (μm)	10.81
$d_{50}$ (μm)	606.29
$d_{90}$ (μm)	908.69
$d_{97}$ (μm)	999.10

In order to determine the changes in the surface morphology after the grinding process, the SEM images of the samples were taken by using a Scanning Electron Microscope (LEO 1430 VP model) after the coverage of the sample surfaces with carbon prior to analysis.

### Oil absorption

A 1 g sample of ground talc was placed on a dry and clean glass plate of 45×45 cm in size. First, a solid paste was prepared by dropping linseed oil from a burette onto the talc powder sample, and mixed with a spatula. Second, the obtained paste was thinned by slow addition linseed oil, and it was spread onto a glass plate as a thin film by using a spatula. The coating process was carried out until no cracking or swelling was observed. Finally, the amount of consumed oil was recorded from a burette in cm<sup>3</sup>, and % oil absorption value of the talc sample was calculated (DIN EN ISO 787-5).

#### Contact angle measurement by sessile drop method

After the drying process of the ground solid samples in an oven at 105 °C, the discs having 2 cm in diameter were prepared by using a manual hydraulic press (Specac GS15011). The labelled discs were kept in a desiccator until the contact angle measurements were performed. No binding additives were utilized for preparation of the disk-shaped test samples. The contact angle of each sample was obtained by using the sessile drop technique at room temperature (25 ± 2 °C) using various polar (water, formamide, and ethylene glycol) and apolar (diiodomethane) liquids with a “KSV Attension ThetaLite TL 101 Optical Tensiometer” instrument. An operation principle

of the instrument is based on addition of a liquid with known surface tension onto a disc with a Hamilton syringe and taking pictures of the drop formed on the solid surface by a video camera. Later, the picture was analyzed, and contact angle was measured by a digital goniometer. Ten different pictures of the droplet were recorded in a very short time interval (millisecond) after the addition of liquid on the solid surface. Finally, the contact angle of each droplet with solid surface was determined, and an average value was obtained by taking arithmetic mean of the contact angle values. This process was repeated on two different points on the disc, and the contact angle values were obtained for the total of three different points. An average of these three values gave the final contact angle value for that liquid. Standard deviation of the measured contact angle values is  $\pm 0.40$  degree.

### Surface Free Energy (*SFE*) calculations

Surface free energy (*SFE*) is a direct measurement of intermolecular forces, and it is defined as the amount of external work done on a material to create a new unit surface area in a vacuum. *SFE* is normally presented in units of  $\text{mJ/m}^2$  (Bhasin et al., 2006; Courard et al., 2011). It is known that *SFE* of solids cannot be determined directly from an experimental measurement. However, it can be obtained indirectly either from wetting heat values obtained from micro calorimeter or contact angle values of solids with various liquids. These two approaches are the most common methods used for this purpose. The results obtained from the contact angle measurements are calculated automatically using different approaches. Some of them were Zisman, Fowkes, Wu, and OCG-Acid Base approaches (Shen et al., 2000). In this study, OCG-AB approach, which is inferred as more appropriate for mineral surfaces was utilized (Zenkiwicz, 2007). Equation 1 defines the OCG-AB method:

$$(1 + \cos \theta) \gamma_L = 2 \left( \sqrt{\gamma_S^{LW} \gamma_L^{LW}} + \sqrt{\gamma_S^+ \gamma_L^-} + \sqrt{\gamma_S^- \gamma_L^+} \right). \quad (1)$$

In Eq.1  $\gamma_L$  represents the total surface energy of the liquid;  $\gamma_S^{LW}$  and  $\gamma_L^{LW}$  show Lifshitz-Van der Walls components of surface energy for solid and liquid, respectively;  $\gamma_S^+$  and  $\gamma_S^-$  represent Lewis electron accepting and donating capacity of solid, respectively;  $\gamma_L^+$  and  $\gamma_L^-$  show Lewis electron accepting and donating capacity of liquid, respectively. The Lewis electron accepting and donating capacity also represents polar component (acid/base) of surface energy for solid or liquid. Consequently, addition of these three components ( $\gamma_S^{LW}$ ,  $\gamma_S^+$ , and  $\gamma_S^-$ ) are formed total surface free energy of the solid. In order to find these three unknowns, it is necessary to measure contact angle of three liquids with known surface energy and its components. In this way, surface energy of solids can be calculated from three equations with three unknown. *SFE* calculations of the ground talc samples were performed by the contact angle measurement instrument automatically using special

software according to OCG-AB methods. Standard deviation of the calculated *SFE* values is  $\pm 0.40$ .

## Results and discussion

### Relationship between particle size and surface area

Only grinding time (5-150 min) was changed during the grinding operations performed in a vibrating ball mill by keeping other parameters constant (Table 3). The particle size distribution (*PSD*) curves of the feed and ground materials are given in Fig. 2, and the change in  $d_{10}$ ,  $d_{50}$ , and  $d_{90}$  grain size of the ground samples are shown in Fig. 3. The results showed that the particle size of talc was reduced with the increasing grinding time in the first 30 min. After 30 min of the grinding time, only a small decrease in the  $d_{90}$  size was observed while other two sizes almost stayed constant. This difference was caused from the longer exposure of coarse particles due to the balls impacts since grinding action was caused from the impact force when the balls were used in a vibrating ball mill as a grinding medium. Similar results were also obtained in literature (Lio and Senna, 1992). The effect of the grinding time on  $d_{50}$  and specific surface area is given in Fig. 4.

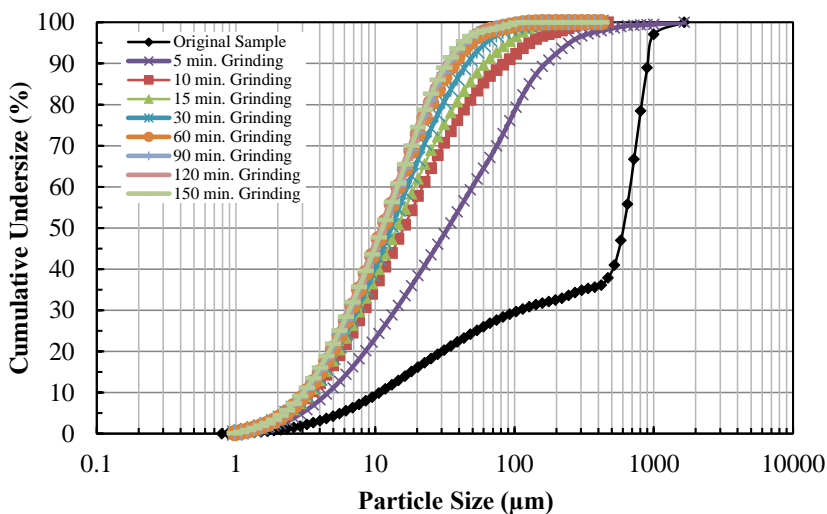


Fig. 2. Particle size distribution (*PSD*) of feed and ground samples

Surface area is a physical property which depends on particle size and porosity of material. Since the available surface would increase with decreasing particle size, an increase in surface area was observed upon grinding. As can be seen in Fig. 4, the decrease in  $d_{50}$  value caused an increase in the surface area of material. Highest surface area ( $18.986 \text{ m}^2/\text{g}$ ) was obtained at the lowest  $d_{50}$  size ( $11.27 \text{ }\mu\text{m}$ ). It is known from the literature that surface area of talc mineral changes between 9.53 to 24.40

m<sup>2</sup>/g with the changing particle size (Holland and Murtagh, 2000; Foster and Doll, 2004). Even there was no a big change in the particle size after 30 min of the grinding time, the surface area of sample kept increasing. This could be explained by conversion of closed pores into open pores and a consequent increase in the total pore volume during the grinding process (Table 4).

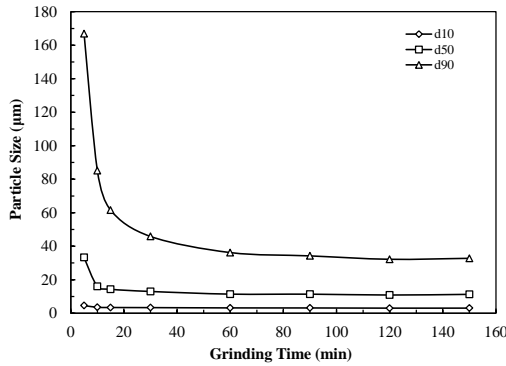


Fig. 3. Change in particle size ( $d_{10}$ ,  $d_{50}$ , and  $d_{90}$ ) with grinding time

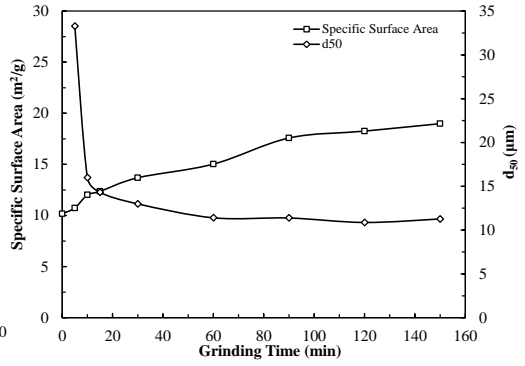


Fig. 4. Changes in  $d_{50}$  size and specific surface area of talc

Table 4. Effect of grinding period on specific surface area, pore volume, color, and oil absorption of talc

Grinding time (min)	Surface area (m <sup>2</sup> /g)	Pore volume (cm <sup>3</sup> /g)	Oil absorption capacity (%)	Contact angle with water (degree)	Color		
					<i>L</i>	<i>a</i>	<i>b</i>
0	10.173	4.162	39.8	63.8	92.05	-0.32	2.4
5	10.734	4.417	43.5	59.3	94.14	-0.26	1.9
10	12.021	4.82	47	60.24	94.70	-0.26	1.94
15	12.361	5.041	48	70.77	94.93	-0.25	1.98
30	13.693	5.548	48.5	65.38	95.22	-0.21	1.83
60	15.027	6.078	50	61.31	96.32	-0.22	2.13
90	17.581	6.836	52.1	63.41	96.41	-0.19	1.97
120	18.256	7.308	52.5	62.05	96.12	-0.12	1.56
150	18.986	7.568	52.7	61.2	95.87	-0.1	1.45

**Effect of grinding on crystallinity**

In order to understand the effect of grinding process performed in the vibrating ball mill on crystal structure of talc, the XRD analyses of samples were performed before and after the grinding process (Fig. 5). Basing on the XRD peak intensities no loss in the crystallinity was observed. However, as it is indicated in a related study in literature, an important amount of crystallinity loss takes place in talc samples after 60 min of grinding in a planetary ball mill (Sanchez-Soto et al., 1997). This discrete



result can be explained by differences in the grinding mechanism of mills. Impact, pressure, and scissors type forces act on particles in vibrating mills. However, pressure and scissors type forces are negligible, and impact is the effective force on grinding. In other words, grinding takes place with impact forces in vibrating ball mills (Stein, 2005; Andres and Haude, 2010).

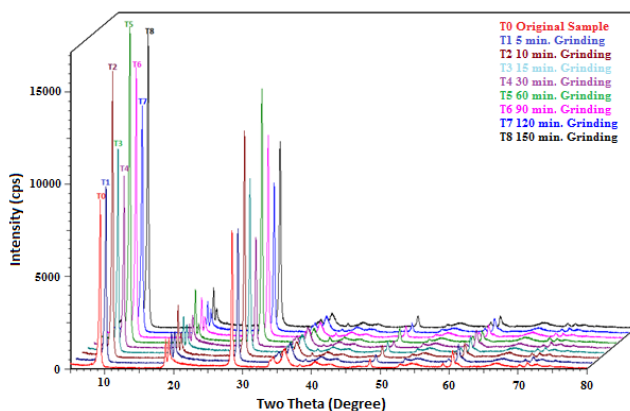


Fig. 5. XRD pattern of feed and ground products

### Relationship between grinding, oil absorption, and contact angle

Knowledge on the oil adsorption value of talc is especially important in paint industry in terms of rheology of paint suspension. Therefore, these tests are routinely performed during production. Oil absorption property of a material depends on various factors such as properties of adsorbent (surface area, pore volume, surface electrical charge, hydrophobicity etc.), structure of adsorbate (ionic/nonionic, HC chain length etc.), and medium conditions (pH, temperature, type and amount of ions etc.) (Bilgin, 2009; Arsoy, 2014; Peng et al., 2014). Table 4 shows that the oil absorption value of talc changes in parallel to the surface area and pore volume. The increasing surface area and opening of the closed pores upon the grinding created more surface for oil absorption. Therefore, talc sample attains maximum oil absorption ratio (52.70%) after 150 min of grinding—where maximum surface area (18.986 m<sup>2</sup>/g) was obtained. It is indicated in literature that sponges (Peng et al., 2014) and cellulose aerogels (Feng et al., 2015) with improved hydrophobic properties showed enhanced oil absorption capacity. However, no logical relation could be established between hydrophobic property and oil absorption capacity of talc in this study. As it can be seen in Table 4, that the highest contact angle (maximum hydrophobic property) was obtained after 15 min of the grinding of talc while its oil absorption value was about 48%. The oil adsorption values of talc products used commercially in industry are between 36% and 52% (Imifabi, 2013). High oil absorption property of talc provides various advantages depending on its usage. According to practical observations, high oil absorption value provides appropriate rheological properties, and adjusts viscosity of mixtures and

prevents sedimentation in paint and paper industries (Arsoy, 2013). In addition, talc with high oil absorption properties increases print quality in paper and cardboard coating processes by balancing ink absorption (Arsoy, 2013). It is desired that clays used in paper coating, paint production, cardboard coating, and relative applications should have appropriate color besides mineralogical purity and a certain particle size distribution (Gamiz et al., 2005).

### Relationship between grinding and color

As known from literature, the whiteness of talc directly affects its usability in cosmetics, paint, and paper industries (Soriano et al., 2002). A color of a substance changes with its chemical/mineralogical structure, grain shape/size, and surface porosity (Bizi et al., 2003; Bilmeyer and Saltzman, 1981). Color properties of powder samples are calculated from its  $X$ ,  $Y$ , and  $Z$  tristimulus values according to the CIE (International Commission on Illumination) color space system, which is given in Fig. 6 as  $L$ ,  $a$ , and  $b$  parameters. In this system,  $L$  is a scale for darkness or lightness of a color varying in an interval from white ( $L=100$ ) to black ( $L=0$ ),  $a$  is scale changing from green ( $-a$ ) to red ( $+a$ ), and  $b$  is another scale varying from blue ( $-b$ ) to yellow ( $+b$ ) (Billmeyer and Saltzman, 1981). As it can be seen from Table 4,  $L$  value of talc increases slightly parallel to the decrease in particle size. Color values of the ground talc samples ( $L=95.87\%$ ,  $a= -0.1$  and  $b= -1.45$ ) are considerable close to the values of commercially available talc samples ( $L=96.92\%$ ,  $a=0.37$  and  $b=2.33$ ). The whiteness of Sivas talc is above the desired values given in Turkish standards (TS 10521; Ersoy et al., 2013).

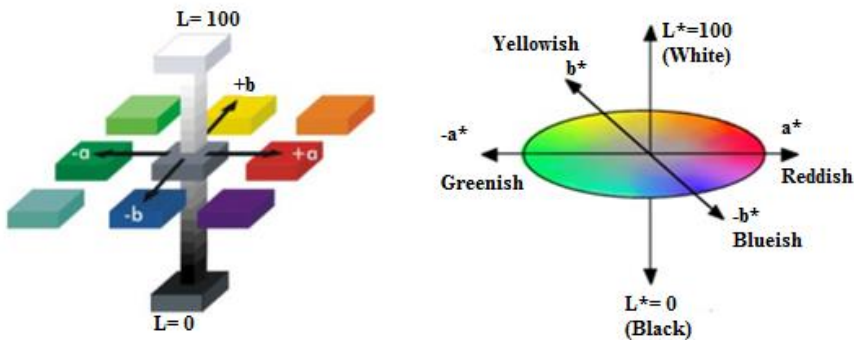


Fig. 6. CIE  $L^*a^*b^*$  color plane (based on Billmeyer and Saltzman, 1981)

### SEM analysis

Secondary electron images of original and ground talc samples obtained from the scanning electron microscope (SEM) are seen in Fig. 7, and fracture mechanism of talc during the grinding process is depicted in Fig. 8. Also, the aspect ratios (the length of basal surface of layer / the thickness of edge surface of layer) of each talc sample were roughly calculated by using the SEM images, and results are presented in

Table 5. The SEM images show that there is an important difference between the particle size and morphology original and ground samples. It can be seen from Table 5 that the sharp corners of talc layers became rounded with the increasing grinding time, and length of layers got smaller upon the grinding (fracture) process. The similar results were already obtained in the previous studies in the literature (Zbik and Smart, 2005; Sanchez–Soto et al., 1997). Especially for first 5 min, it can be said that layers were fractured vertically to the cleavage surface of talc (Figs. 7 and 8), and new layer edge surfaces were formed during the grinding process (Fig.7 a-c and Fig. 8) instead of cleavage of the layers. Correspondingly, the aspect ratio value of samples decreased, and it dropped from 7.8 to 4.5. After 5-15 min of grinding, talc was mostly ground under the direction of the cleavage plane as flakes (Figs. 7d and 8). Therefore, the aspect ratio value reached 19.3 with the increase after 15 min. This is the highest aspect ratio value among all samples, and it is in agreement with the data corresponding highest contact angle (See Fig. 10). It is thought that talc fractured again vertically to the cleavage surface after 15-30 min of grinding process by decreasing aspect ratio (Figs. 7e and Fig. 8, and Table 5). It can be seen in both curves in Fig. 3 and SEM pictures (Fig. 7 f-i) that there is no significant decrease in the particle size of talc, and the particle size stayed almost constant for further grinding time after 30 min. The aspect ratio values in Table 5 support this observation.

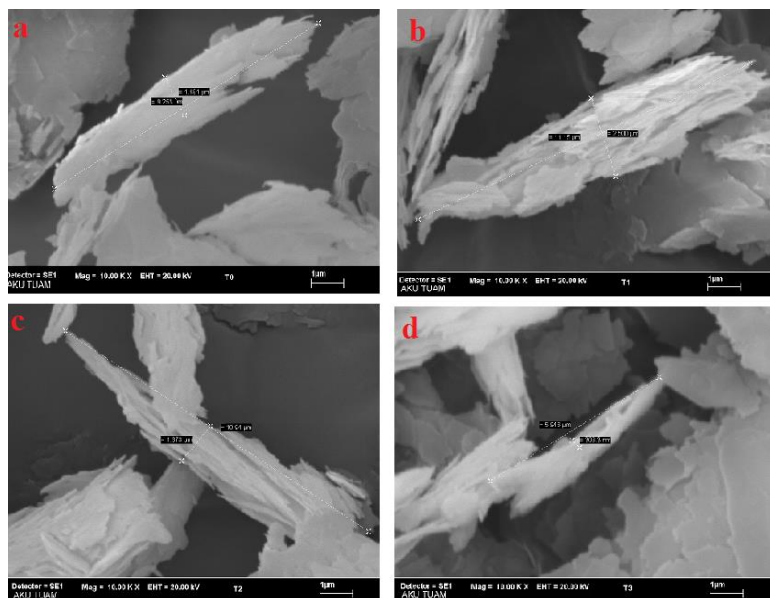


Fig. 7. SEM images of (a) original (-1 mm) talc sample, (b) 5 min, (c) 10 min, (d) 15 min ground talc samples

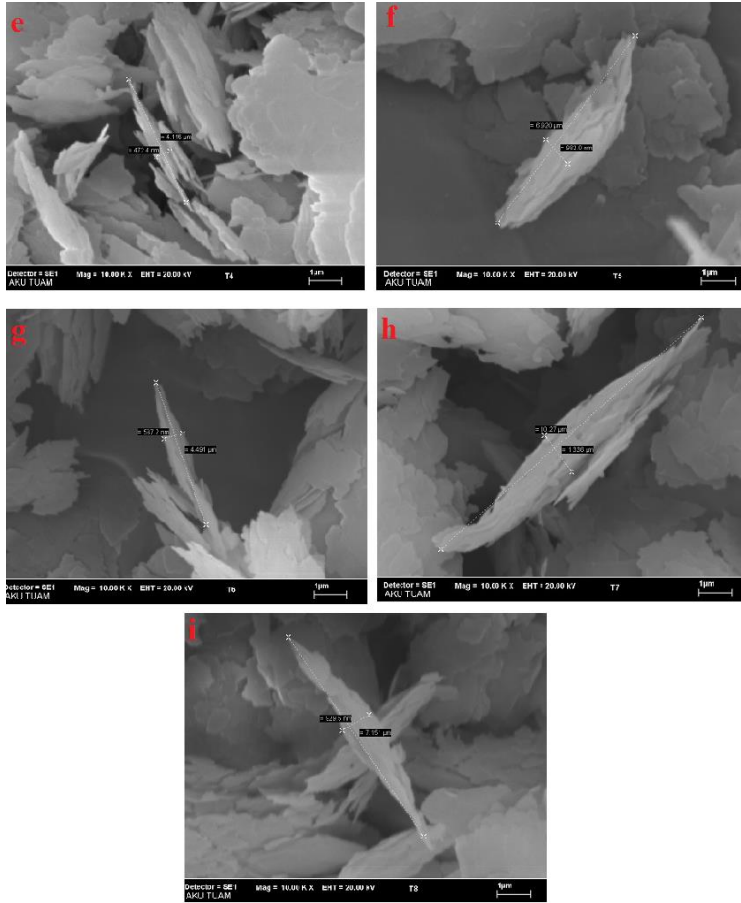


Fig. 7. SEM images of (e) 30 min, (f) 60 min, (g) 90 min, (h) 120 min, (i) 150 min ground talc samples

Table 5. Roughly calculated aspect ratio values of original and ground talc samples obtained from SEM images

Sample code	Grinding time (min)	Aspect ratio (the length of basal surface of layer / the thickness of edge surface of layer)
<i>T0</i>	0	7.8
<i>T1</i>	5	4.5
<i>T2</i>	10	7.9
<i>T3</i>	15	19.3
<i>T4</i>	30	8.7
<i>T5</i>	60	7.1
<i>T6</i>	90	7.6
<i>T7</i>	120	7.7
<i>T8</i>	150	7.7

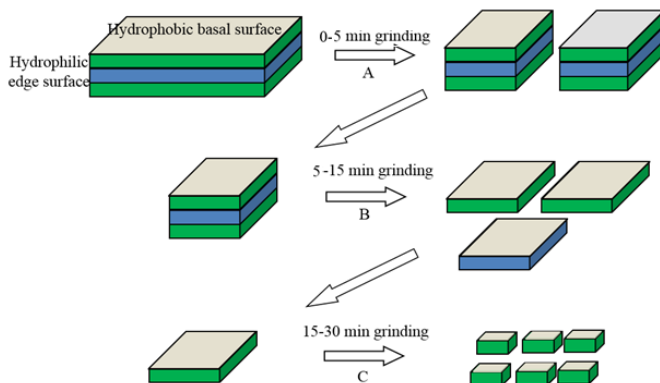
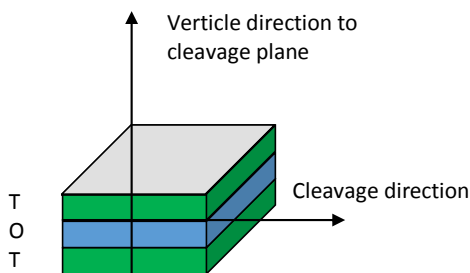


Fig. 8. Fracture mechanism proposed for layered talc in grinding process. A: fracture vertical to the cleavage plane; B: fracture along the layer plane; C: fracture of ground layers again vertical to slicing plane



T : Silica tetrahedral layer  
O : Octahedral (or Brucite) layer

Fig. 9. Layered structure of talc and cleavage direction

### Effect of grinding on contact angle and surface free energy (*SFE*)

Figure 10 shows the changes in the contact angle (with water) and *SFE* of talc with changing the grinding time. The analysis of the curves revealed that our findings are in agreement with the observations in the literature that the hydrophobicity of solids increases and their *SFE* decreases with the increase in their contact angle in the water. On the contrary, this statement is not valid for liquids such as mercury (Drzymala, 1994; Meiron et al., 2004; Sato and Ruch, 1980; Ralph and Nelson, 1988). The contact angle and *SFE* of original talc sample were  $63.80^\circ \pm 0.40$  and  $48.70 \pm 0.40$   $\text{mJ/m}^2$ , respectively. There is a small decrease in the contact angle ( $60.30^\circ$ ), and *SFE* ( $50.50$   $\text{mJ/m}^2$ ) increased slightly in 5 min of the grinding time. After 5-15 min of the grinding time, the contact angle value reached  $70.70^\circ$  with a sudden increase, and *SFE* drop to  $41.80$   $\text{mJ/m}^2$  with a sudden decrease. After 30 min of the grinding time, the contact angle fall to  $65.40^\circ$ , and the *SFE* increased to  $47.50$   $\text{mJ/m}^2$ . These two parameters

stayed almost the same for rest of the grinding time. It is believed that the increase in the contact angle and *SFE* in 30 min is related with a fracture mechanism of talc caused from the change in the “hydrophobic basal surface/ hydrophilic edge surface” ratio. Due to the fracture of talc sample vertically to the cleavage plane (Fig. 9), the contact angle of samples decreased, and the *SFE* increased with the formation of hydrophilic surfaces in the first 5 min of the grinding time.

It is known that surface of talc layers has hydrophobic silanol groups (Si-O-Si), and Mg-OH, and Si-OH groups form hydrophilic edge surfaces (Chiem et al., 2006; Ersoy, 2011). Fracture of talc in the direction vertical to the cleavage plane could be explained by the higher exposure possibility of basal surface of the talc layers to the impacts of balls in grinding media since “hydrophobic basal surface/ hydrophilic edge surface” ratio would be the highest at the beginning. The obtained SEM images support this observation (Figs 7 a-c). During 5-15 min of the grinding time, the layers separated mostly parallel to cleavage direction along with the basal surface by creating new hydrophobic surfaces. Consequently, an increase in the contact angle and a decrease in the *SFE* were observed. This is caused by the increase in the total edge surface area in the prior grinding step and ascending impact of the balls on these edge surfaces. During 15-30 min of the grinding time, vertical fracture to the cleavage plane took place, resulting in new hydrophilic surfaces, decreased contact angle and increased *SFE* as depicted in Fig. 7c.

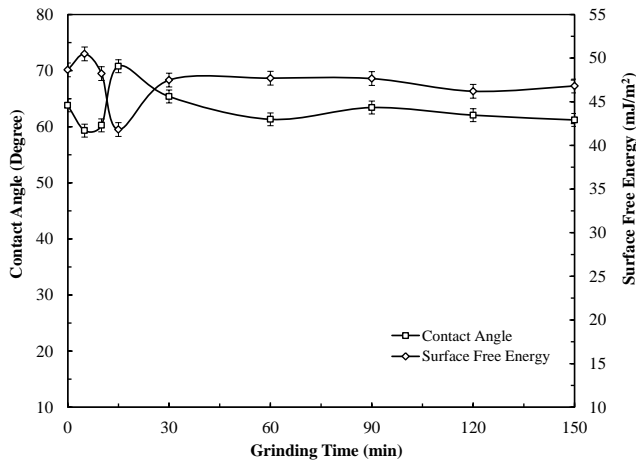


Fig. 10. Change in *SFE* and contact angle of talc with grinding

As stated before, the grinding process over 30 min does not have any important effect on the reduction of talc particle size (Figs. 2 and 3), and both contact angle and *SFE* values stayed almost the same after this period. A similar result was obtained by Terada and Yonemauchi (2004), and a decrease in *SFE* was detected after an increase in the first 10 min of grinding process carried out in a vibrating ball mill during different periods (3, 10, and 40 min.) In the study conducted by Yildirim (2001), it

was observed that the *SFE* and contact angle of two talc samples with different particle sizes were different from each other, and the sample with a smaller particle size showed lower surface and higher contact angle. In a similar study, Malandrini et al. (1997) worked on 3 different talc samples with different talc contents and particle sizes. They obtained lower surface energy and higher contact angle with the increasing talc content and decreasing particle size. Difference between the findings of these two studies and our results is that they are not systematic studies conducted on the same sample for different grinding periods, and obtained from different parts of the samples. Therefore, it is not possible to make one to one comparison between their results and our findings.

## Conclusions

In this study, changes in various physical and surface properties of talc obtained from Sivas in Turkey were followed by applying dry grinding in a vibrating ball mill. The results obtained from this study can be summarized as follows.

Thirty minutes of the grinding time was enough to obtain talc with small particle sizes under the working conditions. Longer grinding periods created a slight increase in the total surface area and pore volume instead of decreasing particle size.

Oil absorption capacity of talc depends on specific surface area, and porosity instead of particle size and hydrophobicity. Highest oil absorption value (52.70%) was obtained with 150 min ground talc sample, which had highest surface area (18.98 m<sup>2</sup>/g).

Effect of grinding on the color of talc is marginal, and whiteness increased in a certain amount while green and yellow values of talc decreased slightly.

The first 30 min of grinding played an important role for both contact angle (thus hydrophobicity) and *SFE* of talc, and no important change occurred for these properties in the consequent grinding time (between 30-150 min). The changes in the hydrophobicity and *SFE* can be explained by fracture mechanism of talc and by consequent changes in the aspect ratio. The SEM images and particle size analysis results supported the proposed mechanism. When talc fractures are vertical to basal plane, the layer surface area/edge surface area ratio of the sample decreases and hydrophilic character increases. If fracture takes place parallel to the cleavage plane, the ratio increases and *SFE* decreases with increasing contact angle and hydrophobic character.

The contact angles of original and ground samples with water were between 59.3<sup>0</sup> and 70.8<sup>0</sup>, and surface free energies were calculated according to Oss-Chaudhury-Good acid-base method were between 48.7 and 41.8 mJ/m<sup>2</sup> range in accordance with the contact angle data. The talc sample with highest hydrophobicity and lowest surface free energy was obtained after 15 min of the grinding time.

The results showed that it was possible to obtain a talc powder with the high aspect ratio value of talc after 30 min of grinding time in a vibrating ball mill (with high

hydrophobicity and low surface energy). It is possible to say that usage of this powder as filler would increase the opacity value of the products in the paint and paper industries. However, a detailed study is needed to make a correlation between hydrophobicity and paint/paper properties.

## Acknowledgement

This study has been supported with a project (12.FEN.BIL.34) provided by Afyon Kocatepe University Scientific Research Projects Coordination Department.

## References

- AGATZINI-LEONARDOU S., TSAKIRIDIS P.E., OUSTADAKIS P., KARIDAKIS T. and KATSIAPI A. 2009, *Hydrometallurgical process for the separation and recovery of nickel from sulphate heap leach liquor of nickeliferous laterite ores*, Minerals Engineering 22, 1181–1192.
- AGLIETTI E.F., 1994, *The effect of dry grinding on the structure of talc*, Applied Clay Science, 9, 139-147.
- ANDRES K. and HAUDE F., 2010, *Application of the Palla™ vibrating mill in ultrafine grinding circuits*, The Journal of The Southern African Institute of Mining and Metallurgy, 110, 125-131.
- ARSOY Z., 2013, *Adacal Industrial Minerals Co., Research and Development responsible*, Research and Development Study Report, 30 p.
- ARSOY Z., 2014, *The Effects of grinding on surface properties of talc (in Turkish)*, Afyon Kocatepe University, Institute of Natural and Applied Science, MS Thesis, p. 101.
- BALEK V., PEREZ-MAQUEDA L.A., POYATO J., CERNY Z., RAMIREZ-VALLE V., BUNTSEVA I.M. and PEREZ-RODRIGUEZ J.L., 2007, *Effect of grinding on thermal reactivity of ceramic clay minerals*, Journal of Thermal Analysis and Calorimetry, 88(1), 87-91.
- BHASIN A., MASAD E., LITTLE D. and LYTTON R., 2006, *Limits on adhesive bond energy for improved resistance of hot-mix asphalt to moisture damage*, Transp. Res. Rec. J. Transp. Res. Board, 1970(1), 3-13.
- BILLMEYER F.W. and SALTZMAN M., 1981, *Principles of Color Technology*, Wiley Interscience, New York.
- BILGIN O., 2009, *Investigation of raw material properties of Gordes zeolites and usability in various industries (in Turkish)*, Afyon Kocatepe, Institute of Natural and Applied Science, PhD Thesis .
- BIZI M., FLAMENT M.P., LETERME PLANNING., BAUDET G. and GAYOT A., 2003, *Relation between structural characteristics of talc and its properties as an antisticking agent in the production of tablets*, European Journal of Pharmaceutical Sciences, 19, 373-379.
- CAWOOD S.R., HARRIS P.J. and BRADSHAW D.J., 2005, *A simple method for establishing whether the adsorption of polysaccharides on talc is a reversible process*, Minerals Engineering, 18(10), 1060-1063.
- CHIEM L., HUYNH L., RALSTON J., and BEATTIE, D., 2006, *An in situ ATR-FTIR study of polyacrylamide adsorption at the talc surface*, Journal of Colloid and Interface Science, 297, 54-61.
- COURARD L., MICHEL F. and MARTIN M., 2011, *The evaluation of the surface free energy of liquids and solids in concrete technology*, Construction and Building Materials, 25, 260-266.
- DELLISANTI F., VALDRE G. and MONDONICO M., 2009, *Changes of the main physical and technological properties of talc due to mechanical strain*, Applied Clay Science, 42, 398-404.



- DIN EN ISO 787-5. *General Methods of Test For Pigments and Extenders – Part 5: Determination of Oil Absorption Value* (ISO 787-5:1980); German Version EN ISO 787-5:1995.
- DRZYMALA J., 1994, *Hydrophobicity and collectorless flotation of inorganic materials*, *Advances in Colloids and Interface Science*, 50, 143-185.
- ERSOY B., 2011, *Influence of pH and chloride-based metal salts on coagulation/dispersion behavior of talc suspension*, *Separation Science and Technology*, 46, 1519–1527.
- ERSOY B., DIKMEN S., YILDIZ A., GOREN R. and ELITOK O., 2013, *Mineralogical and physicochemical properties of talc from Emirdag, Afyonkarahisar, Turkey*, *Turkish Journal of Earth Sciences*, 22: 632-644.
- FENG J., NGUYEN S.T., FAN Z., DUONG H.M., 2015, *Advanced fabrication and oil absorption properties of super-hydrophobic recycled cellulose aerogels*, *Chemical Engineering Journal*, 270 (2015) 168-175.
- FILIO M.J., SUGIYAMA K., KASAI E. and SAITO F., 1993, *Effect of dry mixed grinding of talc kaolinite and gibbsite on preparation of cordierite ceramics*, *JCEJ*, 26, 565-569.
- FOSTER J and DOLL J., 2004, *Particle size effect on talc lubricant activity*, American Association of Pharmaceutical Scientists 2004 annual Meeting Poster Session, 18 p.
- FOWKES F.M., 1964, *Attractive forces at interfaces*, *Industrial and Engineering Chemistry*, 56(12), 40-52.
- FOWKES F.M., 1983, *Acid–base interactions in polymer adhesion: Physicochemical aspects of Polymer Surfaces*, Ed: K.L. Mital, Plenum Press, New York.
- FOWKES F.M., 1972, *Donor–acceptor interactions at interfaces*, *J. of Adhesion*, 4, 155.
- GAMIZ E., MELGOSAB M., SANCHEZ-MARANON M., MARTIN M.J.M. and DELGADOA R., 2005, *Relationships between chemico-mineralogical composition and color properties in selected natural and calcined Spanish kaolins*, *Applied Clay Science*, 28, 269-282.
- GOOD R.J. and VAN OSS, C.J., 1992, *In Modern Approaches to Wettability: Theory and Applications*, Eds: M. E. Schrader, and G. Loeb, Plenum Press, New York, pp. 1-27.
- GOREN R., GOCMEZ H., OZGUR C., 2006, *Synthesis of cordierite powder from talc, diatomite and alumina*, *Ceramics International*, 32, 407-409.
- GRIM R., 1968, *Clay mineralogy*, McGraw-Hill Book Company, New York, 596.
- HOLLAND H.J. and MURTAGH M.J., 2000, *An XRD morphology index for talcs: The effect of particle size and morphology on the specific surface area*, *International Center for Diffraction Data 2000, Advances in X-ray Analysis*, 42, 421-429 p.
- IMIFABI, Talc HTP2, Technical Data Sheet, 2013.
- KANO J. and SAITO F., 1998, *Correlation of powder characteristics of talc during Planetary Ball Milling with the impact energy of the balls simulated by the Particle Element Method*, *Powder Technology*, 98, 166-170.
- KOLLURI O.S., 1994, *Plasma Surface Engineering of Plastics*, ASM Handbook, Vol. 5, Surface Engineering, ASM International, USA.
- LEFEBVRE G., GALET L. and CHAMAYOU, A., 2011, *Dry coating of talc particles with fumed silica: Influence of the silica concentration on the wettability and dispersibility of the composite particles*, *Powder Technology*, 208, 372–377.
- LEJA J., 1982, *Surface Chemistry of Froth Flotation*, Plenum Pres (Second Edition).
- LIAO J. and SENNA M., 1992, *Thermal behavior of mechanically amorphized talc*, *ThermochimicaActa*, 197, 295-306.
- LIU G., FENG Q., OU L., LU Y. and ZHANG G., 2006, *Adsorption of polysaccharide onto talc*, *Minerals Engineering*, 19, 147–153.

- LOPEZ-GALINDO A. and VISERAS C., 2004, *Pharmaceutical and cosmetic applications of clay*, Interface Science and Technology: Clay Surfaces, F.Wypych, K. G. Satyanarayana (Eds.), 1, 267-289.
- MARTIN P.J., WILSON D.I. and BONNETT P.E. 2004, *Rheological study of a talc-based paste for extrusion-granulation*, Journal of the European Ceramic Society, 24(10-11), 3155-3168.
- MEIRON T.S., MARMUR A. and SAGUY I.S., 2004, *Contact angle measurement on rough surfaces*, Journal of Colloid and Interface Science, 274, 637-644.
- NETO J.B.R. and MORENO R., 2007, *Rheological behaviour of kaolin/talc/alumina suspensions for manufacturing cordierite foams*, Applied Clay Science, 3(1-2), 157-166.
- NKOUNBOU C., VILLIERAS F., NJOPWOUO D., NGOUNE C., BARRES O., PELLETIER M., RAZAFITIANAMAHARAVO A. and YVON J., 2008, *Physicochemical properties of talc ore from three deposits of Lamal Pougue area (Yaounde Pan-African Belt, Cameroon), in relation to industrial uses*, Applied Clay Science, 41, 113-132.
- PEREZ-RODRIGUEZ J.L. and SANCHEZ-SOTO P.J., 1991, *The influence of the dry grinding on the thermal behaviour of pyrophyllite*, Journal of Thermal Analysis, 37, 1401-1413.
- PENG L., YUAN S., YAN G., YU P., LUO Y., 2014, *Hydrophobic sponge for spilled oil absorption*, J. APPL. POLYM. SCI., 131(20), 15.
- RALPH D. and NELSON J.R., 1988, *Dispersing powders in liquids*, 245 p., Delaware, U.S.A.
- SANCHEZ-SOTO P.J., WIEWIORA A., AVILES M.A., JUSTO A., PEREZ-MAQUEDA L.A., PEREZ-RODRIGUEZ J.L., BYLINA P., 1997, *Talc from Puebla de Lillo, Spain. II. Effect of dry grinding on particle size and shape*, Applied Clay Science, 12, 297-312.
- SATO T. and RUCH R., 1980, *Stabilization of Colloidal Dispersions by Polymer Adsorption*, 155 p., New-York.
- SHEN W., FILONANKO Y., TRUONG Y., PARKER I.H., BRACK N., PIGRAM P. and LIESEGANG J., 2000, *Contact angle measurement and surface energetic of sized and unsized paper*, Colloids and Surfaces A: Physicochemical and Engineering Aspects, 173, 117-126.
- SORIANO M., SANCHEZ-MARANON M., MELGOSA M., GAMIZ E. & DELGADO R., 2002, *Influence of chemical and mineralogical composition on colour for commercial talcs*, Color Research and Application, 27, 430-440.
- STEIN J., 2005, *Ultrafine dry grinding with media mills*, Post Script Bild Phyphlogo Kleineps, 17(6), 1-6.
- TEMUJIN J., OKADA K., JADAMBAA T.S., MAC KENZIA K.J.D. and AMARSANAA J., 2003, *Effect of grinding on the leaching behaviour of pyrophyllite*, Journal of the European Ceramic Society, 23, 1277-1282.
- TERADA K. and YONEMOCHI E., 2004, *Physicochemical properties and surface free energy of ground talc*, Solid State Ionics, 172, 459-462.
- TOMAINO G.P., 2000, *Talc and pyrophyllite*, Mining Engineering, 64-65.
- TS 10521, December 1992. *Talc-used in paper industry*, Turkish Standard Institute, Ankara (in Turkish).
- ULUSOY U., 2008, *Application of Anova to image analysis results of talc particles produced by different milling*, Powder Technology, 188, 133-138.
- VAN OLPHEN H., 1977, *Clay Colloid Chemistry* (second edition), John Wiley & Sons Inc., New York, 318 p.
- WALLQVIST V., CLAEISSON P.M., SWERIN A., SCHOELKOPF J. and GANE P.A.C., 2009, *Influence of wetting and dispersing agents on the interaction between talc and hydrophobic particles*, Langmuir, 25(12), 6909-6915.

- WANG J. and SOMASUNDARAN P., 2005, *Adsorption and conformation of carboxymethylcellulose at solid-liquid interfaces using spectroscopic, AFM and allied techniques*, Journal of Colloid and Interface Science, 291, 75-83.
- WU W., GIESSE, R.F., Jr. and VAN OSS C.J., 1996, *Change in surface properties of solids caused by grinding*, Powder Technology, 89, 129-132.
- YEKELER M., ULUSOY U. and HICYILMAZ C., 2004, *Effect of particle shape and roughness of talc mineral ground by different mills on the wettability and floatability*, Powder Technology, 140, 68-78.
- YILDIRIM I., 2001, *Surfaces free energy characterization of powders*, Doctor of Philosophy In Mining and Minerals Engineering, Faculty of the Virginia Polytechnic Institute and State University. Blacksburg, Virginia, USA.
- YOON R.H. and YORDAN J.L., 1991, *The critical rupture thickness of thin water films on hydrophobic surfaces*, J. of Colloid and Interface Science, 146,(2), pp. 101-108.
- YANG H., DU C., HU Y., JIN S. YANG W., TANG A., AVVAKUMOV E.G., 2006, *Preparation of porous material from talc by mechanochemical treatment and subsequent leaching*, Applied Clay Science, 31, 290-297.
- ZBIK M., SMART R., ST. C., (2005), *Influence of dry grinding on talc and kaolinite morphology: inhibition of nano-bubble formation and improved dispersion*, Minerals Engineering, 18, 969-976.
- ZENKIEWICZ M., 2007, *Methods for the calculation of surface free energy of solids*, Journal of Achievements in Materials and Manufacturing Engineering, 24, 137-146.